Applied Mathematics, 2020, 11, 146-156
https://www.scirp.org/journal/am
ISSN Online: 2152-7393
ISSN Print: 2152-7385

A Mathematical Model for Redshift

Peter Y. P. Chen

School of Mechanical and Manufacturing Engineering, University of New South Wales, Sydney, Australia
Email: peterypchen@yahoo.com.au

How to cite this paper: Chen, P.Y.P. (2020) A Mathematical Model for Redshift. *Applied Mathematics*, **11**, 146-156.
https://doi.org/10.4236/am.2020.113013

Received: June 4, 2019
Accepted: March 7, 2020
Published: March 10, 2020

Abstract

We have used model scaling so that the propagation of light through space could be studied using the well-known nonlinear Schrödinger equation. We have developed a set of numerical procedures to obtain a stable propagating wave so that it could be used to find out how wavelength could increase with distance travelled. We have found that broadening of wavelength, expressed as redshift, is proportional to distance, a fact that is in agreement with many physical observations by astronomers. There are other reasons for redshifts that could be additional to the transmission redshift, resulting in the deviation from the linear relationship as often observed. Our model shows that redshift needs not be the result of an expanding space that is a long standing view held by many astrophysicists. Any theory about the universe, if bases on an expanding space as physical fact, is open to question.

Keywords

Redshift, Mathematical Modelling, Model Scaling, Nonlinear Schrödinger Equation, Numerical Solution, Stable Propagating Waves

1. Introduction

Shift of spectral lines in the light spectrum from distance stars has been extensively observed and measured by researchers over many centuries. The current most acceptable model is based on Hubble's law which was started from observations of the linear relationship between the velocity and distance of stars. If Doppler Effect due to velocity is taken into consideration, it could be shown that redshift is directly and approximately related linearly to the distance from the stars to the observers.

One of the problems with Hubble model is the large redshifts observed in quasars. Quasar ULAS J1342+0928 is known to have a redshift of 7.54, which corresponds, according to Hubble model, to a distance of approximately 29.36 billion light-years from Earth (these distances are much larger than the distance light could travel in the universe's 13.8 billion year history). Also, based on this theory, recessional velocity of an object is proportional to the distance from observers; it means that for a distant object, its velocity could not just greater than but also hundreds or more times the speed of light. Mathematically, there is no problem to used recessional velocity, based on the assumption of an expanding space between an object and its observers; this conception is, however, difficult to be accepted physically. Many would find it difficult to understand the difference between peculiar velocity, the velocity at which an object moves through space, and recessional velocity.

There is a different theory that is much less known and much less accepted by researchers. This is known as "Tired Light" theory [1]. The idea behind this theory is that, when light is travelling through the cosmic space, it must lose energy through interaction with particles, mostly hydrogen atoms, or other minute particles. Although the space is very thinly populated by those particles, the cumulating effect through an exceedingly long cosmic distance must result in a detectable loss of energy that is manifested itself as redshifts. The proposed theory is that the loss varies exponentially from distance travelled. Although there are qualitative arguments presented on how the loss could have taken place, there is no concrete evidence from laws of physics that such an exponential relationship should exist. Therefore, this theory is closer to just being an empirical correlation between the observed redshifts and distance.

In this paper, we accept the fact that the space is not a complete vacuum. Light as a form of electromagnetic waves in their propagation through space must interact with whatsoever material present, no matter how thinly it is distributed. The transmission is therefore governed by the well-known nonlinear Schrödinger equation (NLSE). We accept the fact that we are dealing with distances not just measured in light year but it could be in billions of light years. If SI units are used, we would be solving NLSE with system parameters as small as 10^{-10} or less. However, these should not be any problems as we could use well-established modelling technique of scaling so that we are solving the scaled-down NSLE with much more convenient numbers. Numerical experiments could then be carried to determine the intrinsic physical properties of the system, in this case the cosmic space. In this paper, we are interested to study the fact that electromagnetic waves are known to increase in their pulse widths when propagating through a medium with anomalous dispersion (that is with a positive dispersion coefficient) [2]. We believe that this is the physical explanation of the universal observation of redshifts (or blue-shift if the coefficient is negative).

Since 1931, the linear relationship between redshift with velocity had received popular support due to Hubble's astronomical observations on nearby stars. However, the present-day theory under the same name is involving so-called recessional velocity that is associated with a yet unproven expanding space. Although there are extensive references, discussions and reviews on this theory, we do not include any reference about them in this paper because we are presenting a completely new transmission model that is based on established physical laws and has not been studied by any researcher on this topic.

There is no dispute that NLSE is the field equation that governs how light waves are propagating through space. In recent years, NLSE is widely used in the development of optical fiber technology. But NLSE is a robust equation that allows the transmission of all sorts of waves under many different conditions. Under this scenario we consider that research works done on the solutions of NLSE are not appropriate for our purpose. We need to know precisely how wavelength changes due to the distance travelled. We do not refer to other researchers' work because our method is unique and aimed at the needs of our model.

2. The Nonlinear Schrödinger Equation (NLSE)

The propagation of light in a medium is governed by the NLSE:

$$u_x - \frac{i}{2} D(x) u_{tt} - i\gamma |u|^2 u = 0 \tag{1}$$

where u is the slow varying envelope of the axial electric field, $D(x)$ and γ represents the dispersion coefficient and self-phase modulation parameters, respectively, x and t is the propagation distance and time, respectively.

Introducing scaling factors, x_o and t_o, so that

$$x^* = \frac{x}{x_o}, \quad t^* = \frac{t}{t_o} \tag{2}$$

Equation (1) becomes

$$u_x - \frac{i}{2} D(x) u_{tt} - i |u|^2 u = 0 \tag{3}$$

where the superscript * has been omitted for simplicity and

$$D^* = \frac{D x_o}{t_0^2}, \quad u^* = (\gamma x_o)^{0.5} u \tag{4}$$

3. The Numerical Solution Method

We have used the Lanczos-Chebyshev pseudospectral reduction method [3] [4] to convert Equation (3) into a set of ordinary differential equations (ODE). Because the emission is a soliton pulse, we need to subdivide the computational t-domain into N divisions. Additionally, a high $(M-1)^{\text{th}}$-order power series for each sub-domain must be used in order to be able to capture the characteristics of the pulse. The resultant ODE is in the form,

$$\boldsymbol{A} U_x(x) - i\boldsymbol{L}\boldsymbol{U}(x) = i\boldsymbol{Q}(x, \boldsymbol{U}) \tag{5}$$

where $\boldsymbol{U}$ is a $(M \times N)$ vector consisting of the coefficients of the power series used. For numerical integration in the x-direction, we have used the unconditionally stable and implicit Crank-Nicholson step-wise formulation. For Equation (5) with step size Δx,

$$\boldsymbol{A}\left(U^{m+1} + U^m\right) - \frac{i\Delta x}{2}\left[\boldsymbol{L}\left(U^{m+1} + U^m\right)\right] = \frac{i\Delta x}{2}\left[\boldsymbol{Q}\left(x, U^{m+1}\right) + \boldsymbol{Q}\left(x, U^m\right)\right] \tag{6}$$

Because the term $\boldsymbol{Q}\left(x,U^{m+1}\right)$ in the LHS, Equation (6) is nonlinear, it has to be solved by an iterative procedure as described in Reference [4].

4. Stable Propagating Wave (SPW)

When applying to a given system, Equation (4) could support the stable wave propagation. Such a wave must have definite pulse energy and the correct pulse shape. The characteristics of SPW are an unchanging pulse shape and slow varying maximum amplitude when travelling along the propagation distance. Any noncompliant components present in the input wave would be dissipated and disappear progressively. However, if the input wave is too far different from a SPW, instability may occur.

Since light emitted from a cosmic object must have travelled through such a long distance, we belive that all the spectral components we received on earth are SPWs. This is feasible as we could find in multi-mode optical fibre technology that the same fiber can support multiple numbers of modes. From multiplex technology, we know that a multiple number of signals can be launched into the same fiber. Therefore, it is logical that we could choose one of the SPWs, for example, that of the hydrogen spectral line H_α, and its associated changes in wave length to find out the extent of redshift.

For the generation of SPWs, we have used numerical procedures that we had developed and used previously. We could find stationary solutions of NLSE for dispersion management in optical fibers [2]. The idea is that we could use a fiber consisting of numbers of segments, each of them has the same dispersion map, for example, half has a positive dispersion coefficient and the other half a negative one. If we take the average of the input and output waves in a segment, after adjustment for any phase change, and use it as the input to the next segment, after a small number of segments, we could obtain a stationary solution quite quickly, providing the initial input pulse is well chosen.

For our numerical model, we have chosen a dispersion map with the first half a dispersion coefficient D and the other half – D, giving 0 as the average coefficient. The reason for this choice is that the physical dispersion coefficient for the cosmic space is very close to zero. For such a dispersion map, there is a zero nett dispersion effect on the travelling wave. However, because of the presence of the nonlinear term in the NLSE, we would not get a stationary solution but a SPW.

It should be noted that in this arrangement the input to each segment is not a solution of NLSE because the input is the phase-adjusted average of the input and output of the previous segment. Therefore, it will take a short distance before the pulse evolves into a SPW.

An example of how a SPW is propagating through a segment is shown in **Figure 1**.

5. Numerical Investigation

For numerical solutions of Equation (3), we consider a pulse at the centre of a

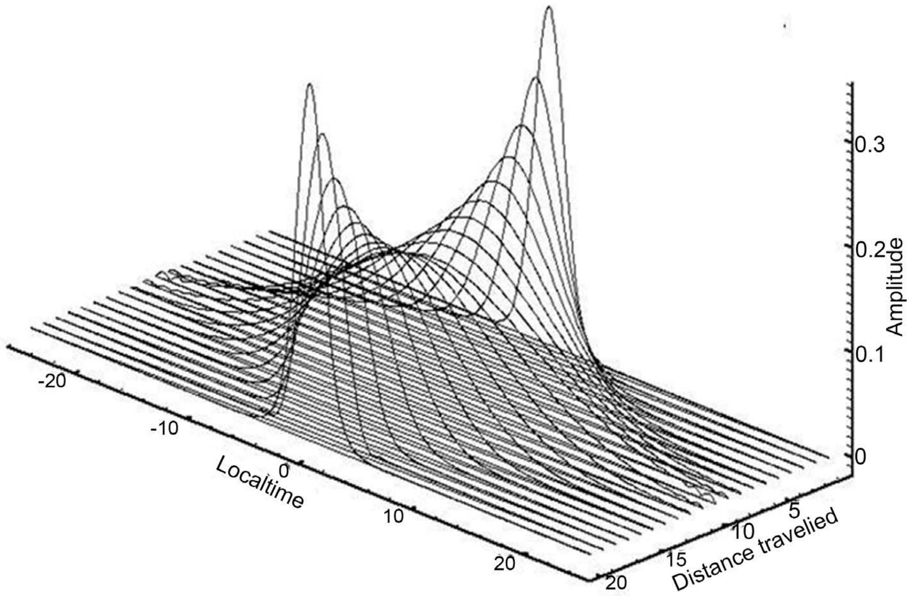

Figure 1. An example of a SPW travelling through a test segment.

local time, t, window between $-L$ to L and travelling in the x direction. We divide this time space into N subdivisions. In each subdivision, u is represented by a $(M-1)^{\text{th}}$ order power series that has M coefficients. The numerical simulation of the propagation of u along x is carried out using step size, Δx. For every $2x$ distance travel, the dispersion coefficient D is positive for the first x distance and $-D$ for the next x distance. We adjust u at the end of each $2x$, according to the procedures described previously. A Gaussian pulse is used as initial input with total pulse energy

$$E = \int_{-L}^{L} \left|u(t)\right|^2 \mathrm{d}t \tag{7}$$

As an example, we use $L = 30$, $N = 4$, $M = 20$, $\Delta x = 0.001$, $x = 1$, $D = 1$ and E =0.25. Changes to the wavelength are found from W, the pulse width at half of the maximum intensity (FWHM). Results for W found numerically are plotted in Figure 2.

Our numerical investigations reveal that the pulse requires a high order polynomial representation. There could be a loss of accuracy if the order is too high. Dividing a given t-domain into numbers of subdivisions could be a workable approach. The choice of the size of a numerical window is also important as the pulse is a narrow spike with long tails. But the pulse width is expanding along the propagation distance. There is a numerical limit on the distance as the window used could become too small for the broadened pulse involved.

For the numerical example described above, a distance of $x = 40$ has been found a limit. For any longer distance, the pulse needs to be re-launched into a larger window in order to cater for the larger pulse width. However, as to be described in the next section, this measure may not be required because re-scaling and calibration could be used to change x to represent any larger distance.

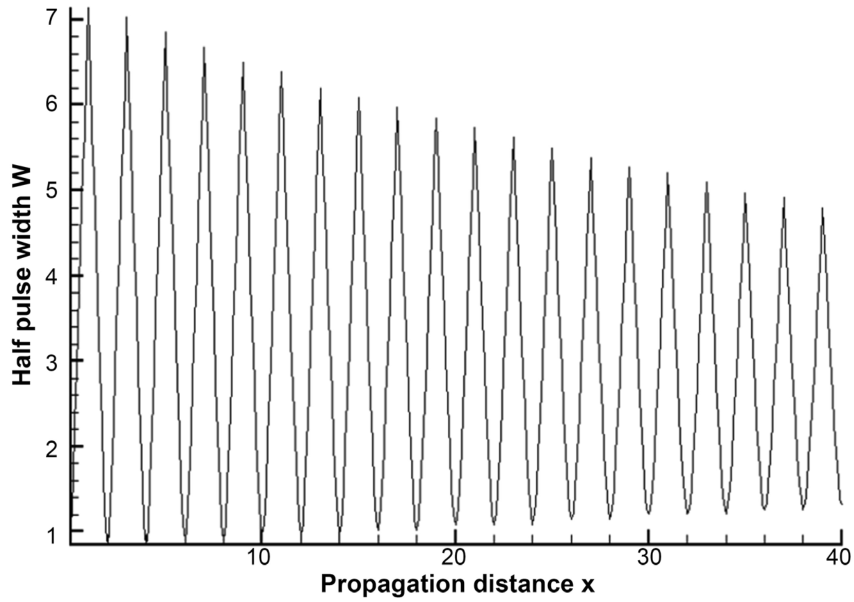

Figure 2. FWHM histories for 20 test segments at $x = 2$ each (Other parameters given in the text).

6. Calibration

As commonly used in model studies, parameters involved could be determined by calibration. We have chosen one of the transmission cycles in **Figure 3** to show how we could use our results to measure redshift in star light as observed on earth. **Figure 3** shows the particular SPW cycle started at $x = 30$. If the initial few steps are ignored we can see that W has an almost exactly linear relationship with x. As Hubble constant, H_o, is determined from physically observed data to represent the linear relationship between redshift and distance, we could calibrate our results based on Hubble's theory:

$$\frac{d}{c} = \frac{z}{H_o} \tag{8}$$

where d is the distance in Mpc, c the speed of light in km·s^{-1}, z the redshift (dimensionless) and H_o in km·s^{-1}·Mpc^{-1}. The usual definition for z is that

$$z = \frac{\lambda_{obs} - \lambda_{st}}{\lambda_{st}} \tag{9}$$

where λ is the wavelength and the subscripts refer to "observed" and "starting" respectively. Since z is a dimensionless ratio, we could define it, using the assumption that λ is proportional to W:

$$z = \frac{W_2 - W_1}{W_1} \tag{10}$$

where the subscript 1 and 2 refer to W measured at x_1 and x_2 respectively. Knowing z, Equation (8) could be used to find the distance d in unit based on what units are used in H_o. In our example as shown in **Figure 3**, W_2 and W_1 are taken at $x_2 = 31$ and $x_1 = 30.5$. Using Equation (10), $z = 0.86$. Using a value of H_o

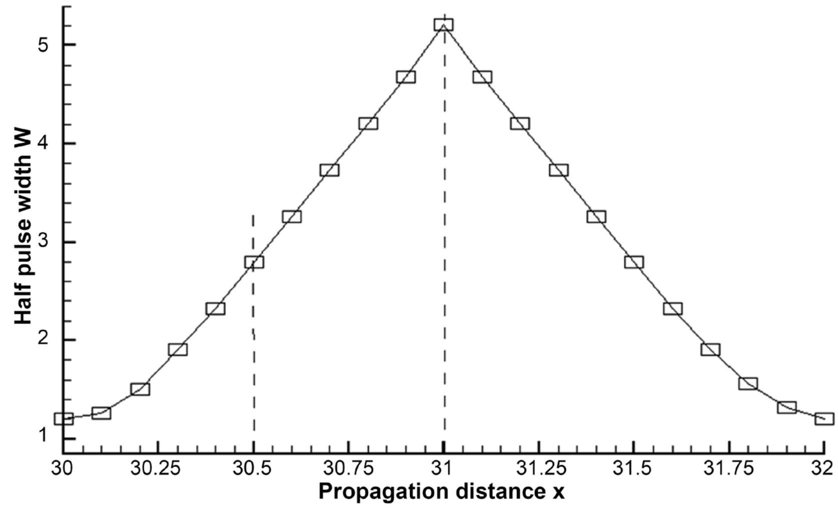

Figure 3. A single test segment is used for calibration.

$= [H_o]_{\text{WMAP}} = 70.3$ in Equation (8) d is found to be 0.01223c Mpc. Since $x_2 - x_1 = 0.5$, we can find the dimensional conversion factor f_d that can be used to convert x to the unit of Mpc (assuming x is dimensionless),

$$(x_2 - x_1) f_d = \frac{d}{c} \tag{11}$$

It should be noted that the dimension in f_d is dependent on the dimension of x. Then, assuming that in this case x is dimensionless,

$$f_d = \frac{d}{c}\frac{1}{x_2 - x_1} = \frac{0.01223}{0.5} = 0.02446\ \text{Mpc} \tag{12}$$

For the local time variable, t, we can find a dimensional conversion factor f_t to convert t into W, the wavelength. If we use Hα spectral line for calibration, the wavelength is 656.281 nm. From **Figure 3**, $W_1 = 2.8$. Therefore, $f_t = 656.281 \div 2.8 = 234.4$ nm (assuming t is dimensionless).

From the calibrations just described, it could be confirmed that our numerical results could be applied for a spectral line of any wavelength.

We could also scale up z so that the results are applicable to a larger distance. Let

$$z^* = f_z z \tag{13}$$

Then, from Equation (8), it could be shown that

$$f_z \frac{d}{c} = \frac{z^*}{H_o} \tag{14}$$

and, from a scale up z^*, a scaled up distance $f_z \frac{d}{c}$ could be found.

7. Further Applications of SPW and Discussions

Readings from **Figure 2**, we can see how W_1 and W_2 change through each computational segment as shown in **Figure 4**. It could be seen that both W_1 and

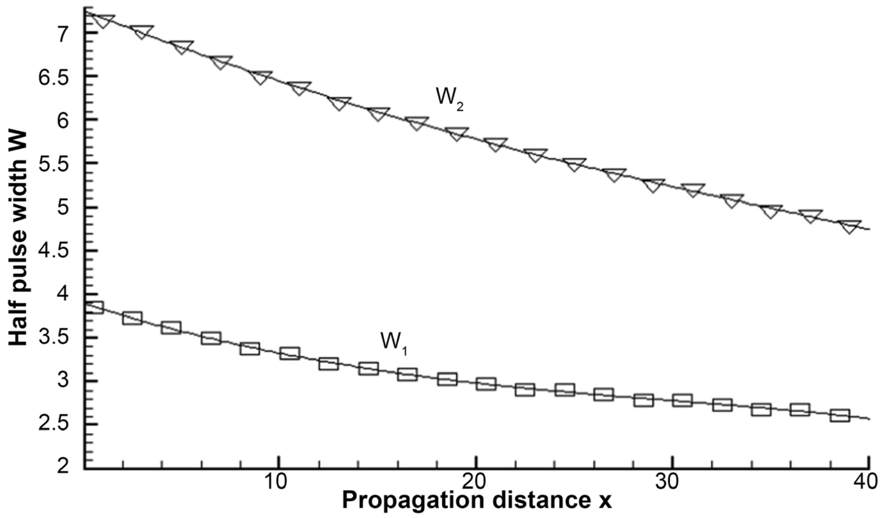

Figure 4. The dependency of output pulse width W_2 with input pulse width W_1.

W_2 are increasing from one segment to the next. Plotting out the corresponding redshift, z, at three selected points is shown in **Figure 5** in that it could be seen that z is slightly increasing with W_1. The implication is for the same system a broader the input wave will lead to a slight increase in z. We have also shown in **Figure 5** that, from the same observed spectrum of a galaxy in the Hubble Deep Field, three observed redshifts for three different wavelengths, H_α, OIII and OII. There is a remarkable agreement between these two sets of data, although they are based on different units. We could see from the previous explanation that scaling in this way is quite acceptable, providing that all the data in a set come from the same system.

So far we have assumed that light waves have come from stationary sources. If they have peculiar velocities, shifts of the spectral lines due to Doppler Effect could be considered as an extra contribution to redshift. Assume all stars at a given distance from earth have randomly distributed radial velocities within a certain range. We have produced a simulated sky map, shown as **Figure 6**, according to the data given in **Table 1**.

This map could be used to explain partly why the Hubble parameter, h, is often given with a specified range.

There are many other events [5], for example, gravitation and an exploding nova that could produce spectral shifts. All could be considered as additional to what we have found.

Although we have found blue-shift in the negative diffusion coefficient segment when we generate our SPW, we do not consider this is the explanation that stars with blue-shift have been observed.

There is no reason to consider this as an exception to the astronomical principle that the universe is uniform and isotropic in every direction. In optical fibers, propagation of light-waves is affected by defects and gaps; light transmission could be abruptly disrupted by environmental conditions. Further research is needed to identify the cause of blue-shift in stars.

Table 1. Data for Sky map simulation.

Distance from earth, Mpc	5	10	15	20
Number of stars	2	4	8	16
Speed range, km·s^{-1}	±20	±40	±70	±100

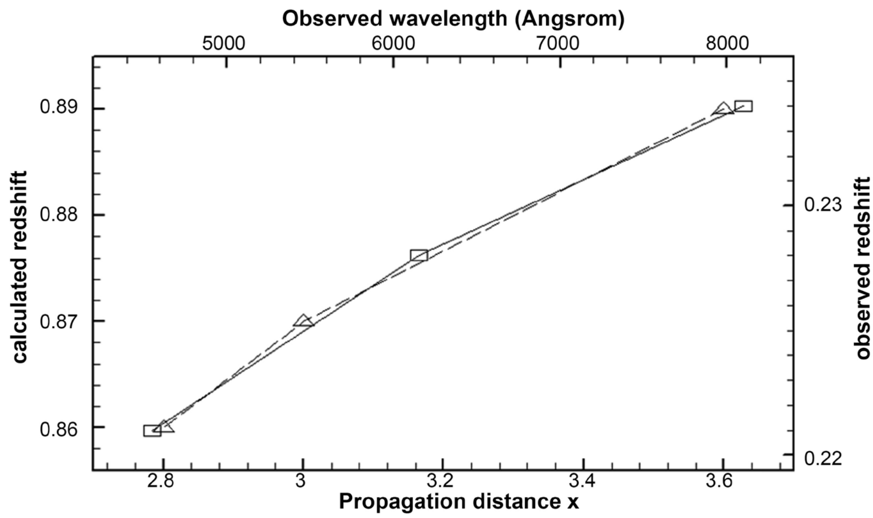

Figure 5. The confirmation of redshift changes with initial pulse width.

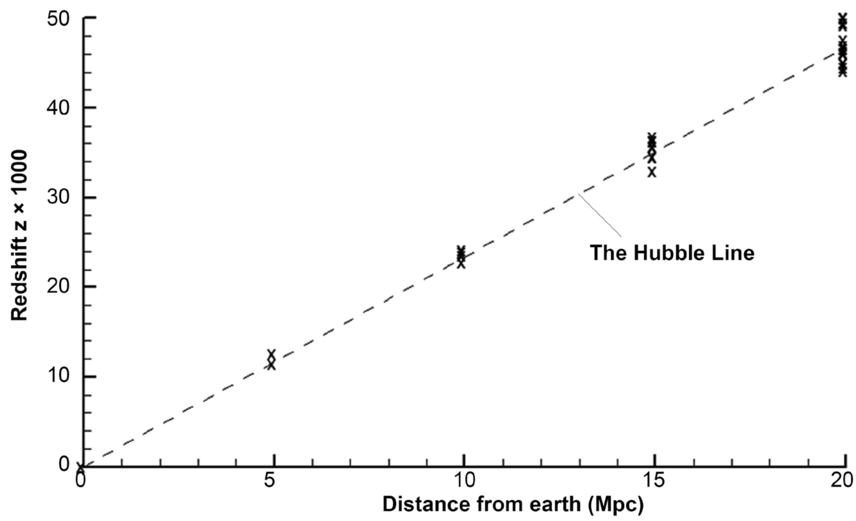

Figure 6. A computer generated sky map.

An important area not covered by this paper is transmission loss. A loss term could be added to NLSE without introducing extra complication to the numerical procedures. On the other hand, our model could be considered to have covered small losses because our system parameters are determined by calibration with observations. For very long distance in many Giga pc, it is worthwhile to consider whether losses should be included as part of the model. The effect of pulse energy is also an area that needs further investigation.

The finding of our numerical investigations based on NLSE is that redshift is linearly proportional to distance measured from the source to earth. There is no limit to this distance. This relationship is completely independent of recessional velocity, if any exists. While our model is not limited by z, the Hubble $z - d$ relationship, as derived originally from Hubble law is applicable only for $z \ll 1$. The fact that this relationship is used for large z is due to its empirical nature. That is H_o is determined from observed data for far distant stars and galaxies.

We acknowledge that as a mathematical tool, in order to account for redshift, it is convenient to assume that the space in which light is travelling is expanding. From observed data, it is possible to work out the relation between the recessional velocities with distance. But we are constantly been reminded that the actual physical distance does not chang. However, there are important cases that have taken the expansion to be real and physical. For example, the Big Bang theory has taken the expansion to be real so that the universe must start from a singular point. Many discussions about the size of our universe have also considered this expansion to be real.

8. Conclusions

We have shown that by using model scaling light propagating through space could be studied by using the well-known NLSE. We have devised numerical procedure to generate SPWs which could be used to show that redshifts commonly observed in light from distant objects could come from the intrinsic physical properties of space, namely dispersion coefficient and self-phase modulation parameter.

Our numerical results confirm that redshift has a linear relationship with distance between a source and our earth. This relationship is not limited by the distance. Our system once calibrated could be applicable to the real physical universe.

Our present model only considers redshift due to light travelling through space. This is known to be the major contribution to redshifts so extensively observed by astronomers. There are other less important causes that could contribute additionally to redshift.

The most important finding in our studies is that redshift needs not come from the recessional velocity of an expanding space. The implication is that any theory about the universe using an expanding space as fact is open to question.

Conflicts of Interest

The author declares no conflicts of interest regarding the publication of this paper.

References

[1] Sho, M.H., Wang, N. and Gao, Z.F. (2018) Tired Light Denies the Big Bang. Redefing Standard Model Cosmology-Intechopen.

[2] Chen, P.Y.P., Malomed, B.A. and Chu, P.L. (2006) Optimal Preprocessing of Pulses

for Dispersion Management. *Journal of the Optical Society of America B*, **23**, 1257-1261. https://doi.org/10.1364/JOSAB.23.001257

[3] Chen, P.Y.P. (2016) The Lanczos-Chebyshev Pseudospectral Method for Solution of Differential Equations. *Applied Mathematics*, **7**, 927-938. https://doi.org/10.4236/am.2016.79083

[4] Chen, P.Y.P. and Malomed, B.A. (2012) Lanczos-Chebyshev Pseudospectral Methods for Wave-Propagation Problems. *Mathematics and Computers in Simulation*, **82**, 1056-1068. https://doi.org/10.1016/j.matcom.2011.05.013

[5] Carroll, A.O. and Ostlie, D.A. (2017) An Introduction to Modern Astrophysics. Cambridge University Press, United Kingdom. https://doi.org/10.1017/9781108380980